Motion of the guest ion as precursor to the first-order phase transition in the cage system GdB_6

Kazuaki Iwasa,* Ryosuke Igarashi, Kotaro Saito, Claire Laulhé,† Toshihiko Orihara, and Satoru Kunii
Department of Physics, Tohoku University, Sendai 980-8578, Japan

Keitaro Kuwahara
Institute of Applied Beam Science, Ibaraki University, Ibaraki 310-8512, Japan

Hironori Nakao and Youichi Murakami
Condensed Matter Research Center and Photon Factory, Institute of Materials Structure Science, High Energy Accelerator Research Organization, Ibaraki 305-0801, Japan

Fumitoshi Iga‡ and Masafumi Sera
Department of Quantum Matter, ADSM & Institute for Advanced Material Research, Hiroshima University, Higashihiroshima 739-8530, Japan, and Institute for Advanced Material Research, Hiroshima University, Higashihiroshima 739-8530, Japan

Satoshi Tsutsui and Hiroshi Uchiyama
SPring-8/JASRI, Sayo, Hyogo 679-5198, Japan

Alfred Q. R. Baron
Materials Dynamics Laboratory, RIKEN SPring-8 Center, Sayo, Hyogo 679-5148, Japan, and SPring-8/JASRI, Sayo, Hyogo 679-5198, Japan
(Received 21 October 2011; revised manuscript received 3 December 2011; published 28 December 2011)

The motion of guest Gd ions in oversized boron cages in GdB_6 was investigated from phonon spectra measurements obtained by inelastic x-ray scattering. The measured phonon modes soften by about 10% from 300 K down to $T_N = 16$ K, in particular, the longitudinal phonon for the propagation vector $\boldsymbol{q}_1 = (1/2,0,0)$ that characterizes the distorted structure below T_N. Besides, the dispersion relation curves show kinklike anomalies at $\boldsymbol{q}_k = (0.38,0.38,0)$. The observed results imply that the motion of the guest Gd ion interplays with the f electrons magnetoelastically and with carriers via Fermi surface nesting. The anomalous properties previously reported for this material far above T_N originate from the strong electron-phonon coupling, which causes the motion of guest ions as precursors to the first-order phase transition.

DOI: 10.1103/PhysRevB.84.214308 PACS number(s): 71.70.Ch, 71.27.+a, 78.70.Nx, 75.80.+q

I. INTRODUCTION

The renormalization of phonons by coupling with other degrees of freedom has been a long-standing subject of interest in condensed matter physics.[1] Conduction electrons, electric dipoles, spin degrees of freedom, etc., contribute to phonon behaviors that are precursors to structural phase transitions. First-order phase transitions without complete freezing phonon modes have been one of the common attractive features,[2,3] in contrast to the complete soft mode concept. In addition, the motion of atoms filled inside oversized cage lattices and their influence on the physical properties have recently become topics of discussion. The anharmonic or off-center motion of the filled atoms has been proposed for reducing the thermal conductivity of high-performance thermoelectricity in clathrate compounds,[4–7] for example. The motion of alkali ions filled in the cage lattice of β-pyrochlore has been proposed to play a role in the superconductivity.[8–10]

We focus on a first-order phase transition system in which the large-amplitude motion of the filled ions may enhance the coupling effects. Rare-earth borides (RB_n, $n = 6,12$, etc.) are ideal for studying such phonon properties because boron atoms form a hard cage and the R ions are interstitially filled inside. Several RB_6 (space group $Pm\bar{3}m$) show flat phonon dispersion relations at around 10 meV, which correspond to R motion in the B cages.[11–15] In GdB_6, the thermal vibration amplitude of the Gd ions is much larger than that of their neighboring boron atoms and those of atoms in other RB_6.[16] GdB_6 undergoes two successive phase transitions with simultaneous structural distortion and antiferromagnetic ordering.[17] At $T_N = 16$ K, a magnetic structure characterized by the wave vector $\boldsymbol{q}_M = (1/2,1/4,1/4)$ (Ref. 18) and a structural modulation by $\boldsymbol{q}_1 = (1/2,0,0)$ are set with first-order phase transition characters. Amara *et al.* proposed the magnetoelastic coupling mechanism by taking into account the Gd ion displacements.[19] This modulated structure is slightly suppressed at $T^* \approx 9$ K, and other modulated structures with $\boldsymbol{q}_2 = (1/2,1/2,0)$ (Refs. 17 and 19) and $\boldsymbol{q}_M$ (Ref. 20) are superimposed. The phonon anomalies' precursors to the complex phase transition in GdB_6 are key for investigating the strong coupling between the large charge fluctuation by the motion of the Gd ions and the electronic degrees of freedom in the cage structure. Such phonon properties would explain the unsolved anomalies in this material. Below 100 K, far above T_N, the spectral width of the electron spin resonance (ESR) increases[21] and the magnetic susceptibility $\chi(T)$ deviates from the Curie law,[22] which is interpreted simply as the formation of short-range magnetic correlation. In heavier R systems, including GdB_6, the lattice-specific heat is in excess at low temperatures.[14]

The excess lattice-specific heat is ascribed to the phonon modes with an energy lower than that expected from the mass difference of R ions.

In this article, we focus on the flat phonon dispersion modes dominated by the Gd ion displacements to gain further insight into the phase transition followed by the high-temperature anomalous behaviors. We present the inelastic x-ray scattering results that reveal the softening and kink features of the phonon modes. These indicate multichannel electron-phonon interactions for the large-amplitude motion of the Gd ions. We present a phenomenological interpretation of the precursor softening based on the Landau-type free-energy function.

II. EXPERIMENTAL DETAILS

We studied two different types of materials: the metallic antiferromagnet GdB_6 and the nonmetallic nonmagnetic system YbB_6 with a Yb^{2+} state.[23] Both samples were synthesized as single crystals by a floating-zone method.[24] The phase transitions in our GdB_6 sample were confirmed by x-ray diffraction and magnetization measurements. We obtained the phonon spectra of GdB_6 by using the inelastic x-ray scattering (IXS) spectrometer installed at BL35XU, SPring-8.[25] The x-ray energy was 21.747 keV generated by a Si (11 11 11) monochromator with backscattering geometry, and a set of 12 analyzers was used to select energy transfers. The energy resolution was about 1.5 meV, and the typical resolution in the reciprocal space was $\Delta \boldsymbol{Q} = (0.06, 0.04, 0.05)$ for the scattering vector $\boldsymbol{Q} = (5.5, 0, 0)$. The phonons of YbB_6 were measured by inelastic neutron scattering (INS). We used the triple-axis spectrometer TOPAN installed at the beam hole 6G of the research reactor JRR-3 in JAEA (Tokai, Japan). The scattered neutron energy was fixed at 30.5 meV. A pyrolytic graphite filter was installed for eliminating higher-order contamination. Three horizontal collimators for beam-divergence angle 30′ were used on the path after the monochromator to the detector. The energy resolution at the elastic position was 2.0 meV, as evaluated from the incoherent scattering profile. The resolution widths in the reciprocal space were estimated as 0.065 r.l.u. and 0.15 r.l.u. within the horizontal scattering plane and along the vertical direction, respectively. In both experiments, the sample temperatures were controlled by helium closed-cycle refrigerators.

III. RESULTS AND ANALYSIS

Figure 1 shows spectra measured at $\boldsymbol{Q} = (5 + \zeta, 0, 0)$ for GdB_6. Pronounced excitation peaks appearing in the range of 5–10 meV are assigned to a longitudinal (L) phonon branch with a propagation vector $\boldsymbol{q} \parallel [100]$. Figure 2 shows dispersion relation curves of the L mode measured at 20 K and 300 K as well as that of YbB_6 at 300 K.

The dispersion relation of GdB_6 near the zone center is consistent with that previously deduced from the ultrasonic measurement, indicated by a dashed line[27] and similar to that of YbB_6. The L-mode energy of GdB_6 reaches a maximum around $\zeta \sim 0.2$, and the dispersion curve bends down to the Brillouin zone boundary $\boldsymbol{q}_1$. This is in marked contrast to the monotonous variation against $|\boldsymbol{q}|$ for YbB_6.[26] The lower-energy branch due to the apparent bending down

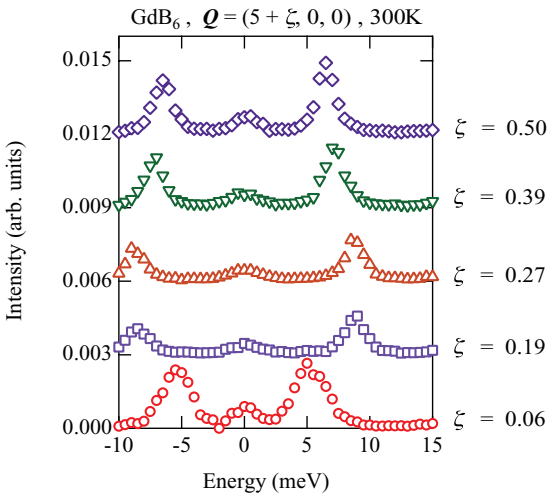

FIG. 1. (Color online) IXS spectra of GdB_6 measured at $\boldsymbol{Q} = (5 + \zeta, 0, 0)$. Each set is shown with a relative shift of the ordinate by 0.003.

can be attributed to the mode dominated by the Gd ion motion, as noted previously. The bending lower-energy branch originates the excess lattice-specific heat[14] and the diffuse x-ray scattering intensities centered at $\boldsymbol{q}_1$, as a result of the integration of the energy spectrum by the laboratory diffractometer.[26] Amara *et al.* proposed that the modulated structure with $\boldsymbol{q}_1$ is composed of the longitudinal displacement of the Gd ion coupled magnetoelastically with the localized magnetic moments of Gd.[19] Thus, the present phonon anomaly addresses the instability of the $\boldsymbol{q}_1$ L mode mediated by the strong interplay with the f electrons. It is consistent with no anomaly of the phonon branch in nonmagnetic YbB_6. Figure 3 shows the temperature dependence of the spectra measured at $\boldsymbol{Q} = (5.5,0,0)$ in GdB_6.

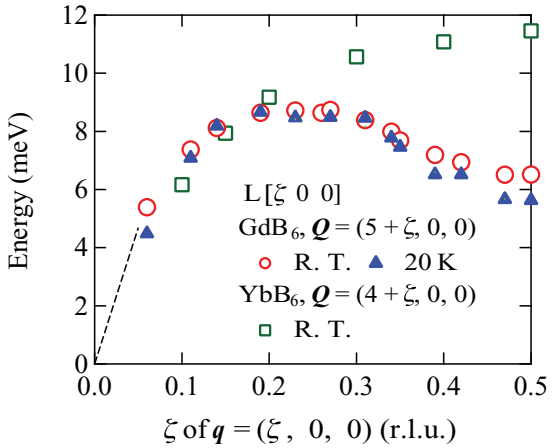

FIG. 2. (Color online) Phonon dispersion relation curves of the L modes propagating along the [100] axis for GdB_6 and YbB_6,[26] which were taken at the different Brillouin zones centered at (5, 0, 0) and (4, 0, 0), respectively. The dashed line represents the dispersion slope determined by ultrasonic measurements for GdB_6.[27] The experimental error bars are smaller than the symbol sizes.

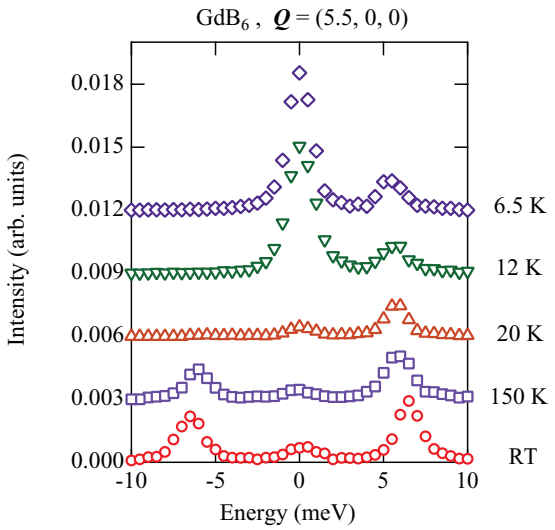

FIG. 3. (Color online) Temperature variation of the IXS spectra at $\boldsymbol{Q} = (5.5, 0, 0)$ of GdB_6. Each set is shown with a relative shift of the ordinate by 0.003.

The elastic peak appearing below T_N is caused by the structural transition.[17,19] It is also remarkable that the L mode shows significant softening down to T_N. A procedure of least-squares fitting of a Lorentzian profile to the observed phonon peak was carried out, and the temperature dependence of the phonon energy squared for $\boldsymbol{q} = (0.47,0,0)$ close to $\boldsymbol{q}_1$ is shown in Fig. 4.

The softening indicates anharmonic potentials for the Gd ion sites and is viewed as a precursor to the magnetic and structural transitions at T_N. The L-mode energy near $\boldsymbol{q}_1$ exhibits softening by 13.1% from 300 K down to T_N, and it increases slightly below T_N. In contrast, no softening of the $\boldsymbol{q}_1$ L mode was observed for YbB_6 in a previous INS experiment.[28]

Next, we consider the phonon branch propagating along the [110] axis. Figure 5(a) shows excitation peaks at around 8 meV for the $\boldsymbol{q} \sim (0.35,0.35,0)$ L mode for GdB_6 measured at 20 K and 300 K.

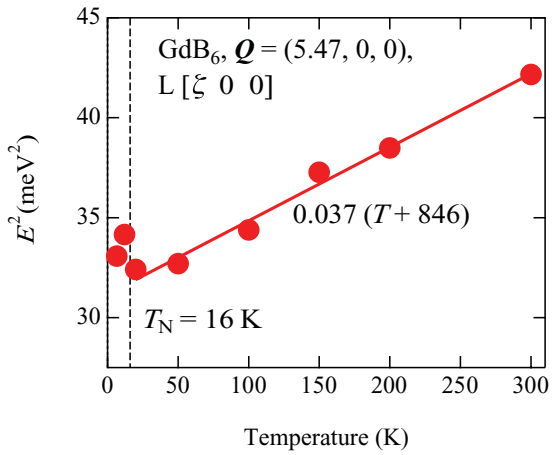

FIG. 4. (Color online) Temperature dependence of the squared energy for the L mode with $\boldsymbol{q} = (0.47,0,0)$ (symbols). A fitted linear function for the data above T_N is shown by the solid line.

This mode softens by 9% from 300 K down to 20 K. The transverse (T) mode with $\boldsymbol{q} \parallel [110]$ exhibits less softening. Similar softening behaviors were reported for $\boldsymbol{q}_2$ of YbB_6 measured by INS (Ref. 28) and SmB_6 measured by nuclear resonant scattering.[29] The softening magnitudes are 2%–3% from 300 K down to 40 K for YbB_6 and down to 150 K for SmB_6, which are smaller than the softening magnitudes of GdB_6. Because this softening is common for these various compounds, we believe that it arises from the anharmonic potentials at the R sites in the oversized cages. However, the larger softening magnitudes for the various modes in GdB_6, as compared to those of other materials, are indicative of the enhancement in the lattice instability in GdB_6.

We move on to investigate the dispersion relations for the [110] L mode. The INS spectra for YbB_6 measured at 300 K are shown in Fig. 5(b), and the dispersion relation curve for the L-mode branch is represented by green squares in Fig. 6.

It follows a smooth curve within the measured Brillouin zone. On the other hand, the dispersion relation of GdB_6 by IXS exhibits a kink anomaly around $\boldsymbol{q}_k = (0.38,0.38,0)$. A similar kink is also observed in the flat dispersion curve of the T mode with $\boldsymbol{q} \parallel [110]$.

IV. DISCUSSION

Hereafter, we discuss the softening $\boldsymbol{q}_1$ L mode, which is considered as the largest precursor anomaly to the first-order phase transition in GdB_6. We use the model for first-order structural phase transitions with slight phonon softening above the transition temperature, discussed by Krumhansl and Gooding taking into account the Landau-type free energy.[2,3] According to their theory, the free-energy function should be expanded with respect to the amplitude of the Gd ion displacement in the relevant mode. The amplitude is defined as $\Psi = A\exp(i\phi)$ for the displacement written as $\boldsymbol{u}(\boldsymbol{r}) = \hat{\boldsymbol{e}}_{[100]} A\sin(\boldsymbol{q}_1 \cdot \boldsymbol{r} + \phi)$, where $\hat{\boldsymbol{e}}_{[100]}$ represents the polarization unit vector. We take into account a simple invariant form of free energy as $F = \frac{a}{2}|\Psi|^2 - \frac{b}{4}|\Psi|^4 + \frac{c}{6}|\Psi|^6$. The coefficients a, b, and c are represented as combinations of magnitudes of magnetic moments, free-energy parameters for the magnetic sector, and magnetoelastic coupling constants, as introduced for the premartensitic transition in a magnetoelastic system Ni_2MnGa (space group $Fm\bar{3}m$).[31] Within the linear response approximation $|\Psi| = \chi_0 B$, where χ_0 and B are the susceptibility and external field, respectively, the free-energy term for the $|\Psi|^2$ order is $|\Psi|B = \chi_0^{-1}|\Psi|^2$. We can assume that the Curie-Weiss law $\chi_0^{-1} \propto (T + T_0)$, and it should be proportional to the coefficient a. In addition, a is ascribed to a force constant for the atomic motion in the harmonic approximation. It is proportional to the squared frequency of the motion (E^2). Therefore, a/c is assumed to be proportional to the squared energy of the renormalized softening phonon, which is expressed as $E^2 = C(T + T_0)$. The experimental data of the phonon energy of the L mode near $\boldsymbol{q}_1$ are reproduced by $C = 0.037$ meV^2/K and $T_0 = 846$ K, as indicated by the solid line in Fig. 4. Next, considering $\frac{\partial(F/c)}{\partial|\Psi|} = 0$ and $\frac{\partial^2(F/c)}{\partial|\Psi|^2} = 0$, we define the characteristic temperatures for the stable states seen in the free-energy curve. For $a/c > b^2/4c^2$ corresponding to the high-temperature region, F/c has only one minimum at

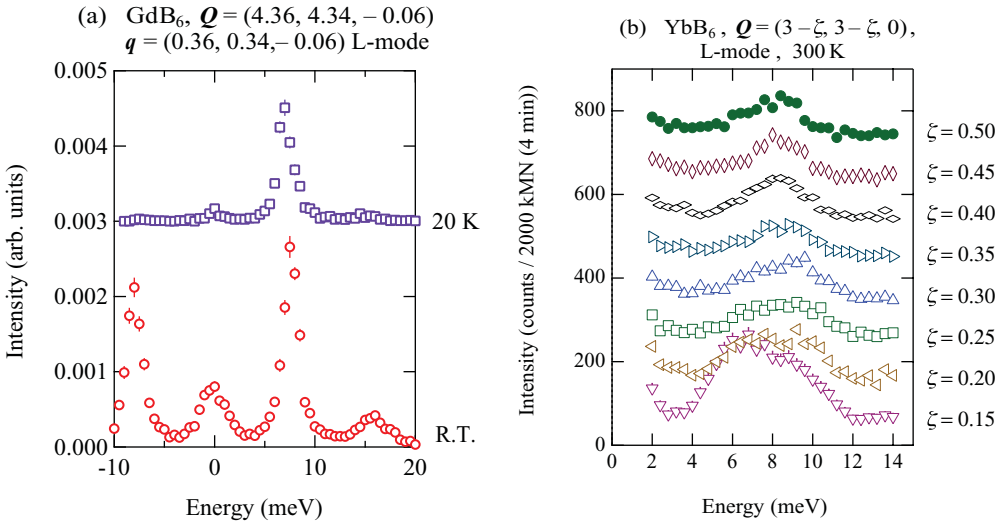

FIG. 5. (Color online) (a) IXS spectra of GdB_6 measured at $\boldsymbol{Q} = (4.36, 4.34, -0.06)$. Each set is shown with a relative shift of the ordinate by 0.003. (b) INS spectra of YbB_6 at $\boldsymbol{Q} = (3-\zeta, 3-\zeta, 0)$. Each set is shown with a relative shift of the ordinate by 100.

$|\Psi| = 0$ as the atomic position. The condition $a/c = b^2/4c^2$ is approached with a decrease in temperature. We define the temperature $T_{\rm inf}$ as $a/c = C(T_{\rm inf} + T_0) = b^2/4c^2$, below which a metastable state with finite magnitude of $|\Psi|$ appears in the free-energy curve. When a/c reaches $C(T_{\rm N} + T_0) = 3b^2/16c^2$ upon a further decrease in temperature, a new stable state at $|\Psi| \neq 0$ appears at $T_{\rm N}$. From these conditions, together with $T_{\rm N} = 16$ K and $T_0 = 846$ K, we obtain $T_{\rm inf} = 303.3$ K and $b/c = 13.0$, and the calculated decrease of phonon energy from $T_{\rm inf}$ to $T_{\rm N}$ is 13.4%. It is almost equal to the experimental result of 13.1% from 300 K to $T_{\rm N}$. Figure 7 shows F/c at $T_{\rm N}$ and $T_{\rm inf}$ calculated from the determined a/c and b/c.

In the measurement-temperature range below $T_{\rm inf}$, with a decrease in the metastable-state energy, the relevant potential for the Gd ion along the [100] axis around $|\Psi| = 0$ gradually deviates from the harmonic potential with only the quadratic term at $T_{\rm inf}$, as indicated by the green dotted line. Considering the Gd ion displacement magnitude of 0.015 Å for the $\boldsymbol{q}_1$ L mode evaluated from the x-ray diffraction data,[19] the height of the free-energy barrier between the two minima at $T_{\rm N}$ is 22 meV. On the other hand, the first excited level for the quantized oscillation at 8 meV is located inside a potential well centered at the stable atomic positions. The second level stays in the energy region of the deformed potential, and the energies of the higher levels are beyond the barrier energy. We propose that the emergence of the metastable state owing to the latter anharmonic softening motion of the guest Gd ions causes the magnetic correlation observed as the anomalies in the ESR linewidth and $\chi(T)$ far above $T_{\rm N}$.[21,22] The softening behavior common for RB_6 indicates that the R ion is located in an anharmonic shallow potential within the boron cage. Among them, the bending down of the [100] L-mode dispersion relation curve in GdB_6 is the most pronounced feature. The strong anharmonicity and softening in GdB_6 originate from the dynamical effect of the magnetoelastic coupling of the large magnetic moments of Gd ions (the angular moment of $J = 7$) with the motion of guest Gd ions in the oversized cage lattice, as proposed in the structural-distortion study.[19] Pairing of the neighboring Gd ions by the atomic displacement with $\boldsymbol{q}_1 = (1/2,0,0)$ might give rise to the gain in magnetic exchange interaction energy. This mechanism is not expected for the nonmagnetic YbB_6 and the less magnetic system SmB_6. A further study on other RB_6 is required to clarify the general effect of the magnetoelastic coupling on their structural dynamics.

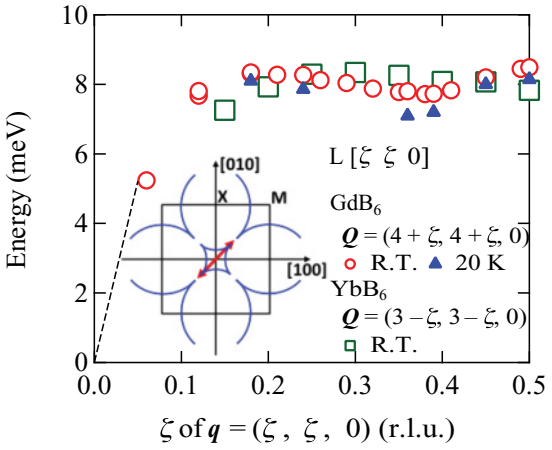

FIG. 6. (Color online) Phonon dispersion relation curves of the L modes propagating along the [110] axis. The dashed line represents the dispersion slope determined by ultrasonic measurements for GdB_6.[27] The inset depicts the Fermi surface shape in the [100]-[010] plane.[30] The experimental error bars are smaller than the symbol sizes.

We observed clearly the kink anomalies in the phonon branches along the $\boldsymbol{q} \parallel [110]$. This feature can be assigned to a Kohn anomaly via the Fermi surface nesting instability because GdB_6 and YbB_6 are metallic and nonmetallic, respectively. This idea is supported by the electronic band calculation studies, which suggest similar shapes of the Fermi surfaces in the metallic RB_6.[32] As depicted in the inset of Fig. 6, four ellipsoidal Fermi surfaces connect with each other through a

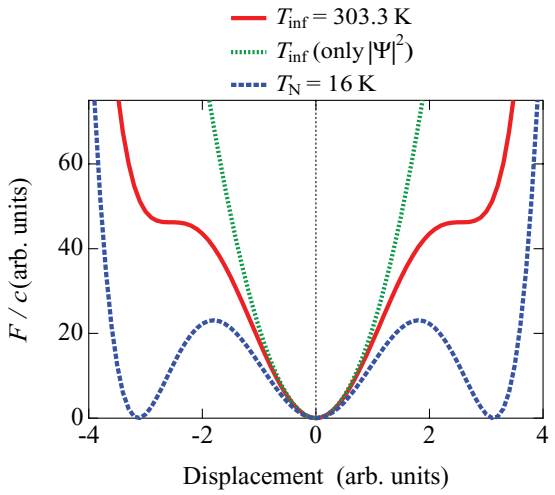

FIG. 7. (Color online) Calculated free-energy functions, $F/c = \frac{a}{2c}|\Psi|^2 - \frac{b}{4c}|\Psi|^4 + \frac{1}{6}|\Psi|^6$, at T_{inf} (red solid line) and T_N (blue broken line). That with only the quadratic term at T_{inf} is shown by a green dotted line. Here, T_{inf} is defined by $C(T_{inf} + T_0) = b^2/4c^2$, below which the metastable state appears at $|\Psi| \neq 0$.

necklike shape surrounding a hole pocket centered at the Γ point within the [100]-[010] plane.[30] The neck is expected to have a nesting condition by the translation vector close to the kink wave vector $\boldsymbol{q}_k$, indicated by the arrow in the inset. Because the observed flat phonon modes around 8 meV are dominated by the Gd motion, the kink is attributed to the coupling between the Gd ion motion and the conduction electrons.

The L- and T-phonon modes for $\boldsymbol{q}_2$, corresponding to the lattice distortion below the lower transition temperature $T^* \approx 9$ K, do not show any singularity, which is in contrast to the $\boldsymbol{q}_1$ L- mode. The transition at T^* accompanies no anomaly in the specific heat,[14] implying that the free-energy change at T^* is much less than that at T_N. Thus, the anomaly of structural dynamics for $\boldsymbol{q}_2$ can be small. Another noticeable point is that the two wave vectors, $\boldsymbol{q}_2$ for the lattice distortion below T^* and $\boldsymbol{q}_k$ for the Kohn anomaly, are close to each other. The instabilities caused by these wave vectors may compete with each other; this results in a less effective instability than that caused by $\boldsymbol{q}_1$. Thus, the transition characterized by $\boldsymbol{q}_1$ occurs at the higher temperature T_N, and the tiny modification of the distortion characterized by $\boldsymbol{q}_2$ is superimposed at lower T^*.

V. SUMMARY

We conclude that the f-electron-phonon interaction considerably deforms the potential and causes significant softening of the Gd motion as a precursor to the first-order phase transition characterized by $\boldsymbol{q}_1$. Besides, the kink behavior at $\boldsymbol{q}_k$ suggests that there exists an effect of carriers on the Gd motion via Fermi surface nesting. The large-amplitude motion of the guest Gd ions in their oversized cages enhances the electron-phonon coupling through these multichannel interactions with the electronic states. The present results provide a method of study of the role of coexisting or competing electron-phonon interactions in the emergence of ordered states from nearly degenerated ground states to low-symmetry lattice structures.

ACKNOWLEDGMENTS

The authors thank M. Kohgi for initiating this study. H. Harima and Y. Kuramoto are acknowledged for their fruitful discussions. K. Tomiyasu and M. Onodera are appreciated for their support at Tohoku University. The study is partially supported by the Grants-in-Aid for Scientific Research from the Ministry of Education, Culture, Sports, Science and Technology (MEXT) of Japan (No. 19540355, No. 20102005, No. 21224048, and No. 23244068) and by JSPS (FIRST Program "Quantum Science on Strong Correlation"). C.L. acknowledges support from the Japan Society for the Promotion of Science (financial support 20·08728 from MEXT). The synchrotron radiation experiments were performed at SPring-8 with the approval of JASRI (2007B1328 and 2009A1224). The neutron scattering experiment at JRR-3 (JAEA, Tokai) was performed under the User Program conducted by ISSP, University of Tokyo.

*iwasa@m.tohoku.ac.jp
†Present address: Synchrotron SOLEIL, Saint Aubin BP48, 91 192 Gif-sur-Yvette, France.
‡Present address: Faculty of Science, Ibaraki University, Ibaraki 310-8512, Japan.

[1] Y. Yamada, *Dynamical Properties of Solids* (North-Holland, Amsterdam, 1984), Vol. 5, p. 329.
[2] J. A. Krumhansl and R. J. Gooding, Phys. Rev. B **39**, 3047 (1989).
[3] J. A. Krumhansl, Solid State Commun. **84**, 251 (1992).
[4] B. C. Sales, B. C. Chakoumakos, R. Jin, J. R. Thompson, and D. Mandrus, Phys. Rev. B **63**, 245113 (2001).
[5] M. Christensen, A. B. Abrahamsen, N. B. Christensen, F. Juranyi, N. H. Andersen, K. Lefmann, J. Andreassons, C. R. H. Bahl, and Bo B. Iversen, Nat. Mater. **7**, 811 (2008).
[6] Y. Takasu, T. Hasegawa, N. Ogita, M. Udagawa, M. A. Avila, K. Suekuni, and T. Takabatake, Phys. Rev. Lett. **100**, 165503 (2008).
[7] T. Mori, S. Goshima, K. Iwamoto, S. Kushibiki, H. Matsumoto, N. Toyota, K. Suekuni, M. A. Avila, T. Takabatake, T. Hasegawa, N. Ogita, and M. Udagawa, Phys. Rev. B **79**, 212301 (2009).
[8] Y. Nagao, J. Yamaura, H. Ogusu, Y. Okamoto, and Z. Hiroi, J. Phys. Soc. Jpn. **78**, 064702 (2009).
[9] H. Mutka, M. M. Koza, M. R. Johnson, Z. Hiroi, J. Yamaura, and Y. Nagao, Phys. Rev. B **78**, 104307 (2008).
[10] T. Hasegawa, Y. Takasu, N. Ogita, M. Udagawa, J. Yamaura, Y. Nagao, and Z. Hiroi, Phys. Rev. B **77**, 064303 (2008).
[11] H. G. Smith, G. Dolling, S. Kunii, M. Kasaya, B. Liu, K. Takegahara, T. Kasuya, and T. Goto, Solid State Commun. **53**, 15 (1985).
[12] P. A. Alekseev, A. S. Ivanov, B. Dorner, H. Schober, K. A. Kikoin, A. S. Mishchenko, V. N. Lazukov, E. S. Konovalova, Yu. B. Paderno, A. Yu. Rumyantsev, and I. P. Sadikov, Europhys. Lett. **10**, 457 (1989).

[13]S. Kunii, J. M. Effantin, and J. Rossat-Mignod, J. Phys. Soc. Jpn. **66**, 1029 (1997).
[14]S. Kunii, T. Takahashi, and K. Iwashita, J. Solid State Chem. **154**, 275 (2000).
[15]K. Takegahara and T. Kasuya, Solid State Commun. **53**, 21 (1985).
[16]Y. Takahashi, K. Ohshima, F. P. Okamura, S. Otani, and T. Tanaka, J. Phys. Soc. Jpn. **68**, 2304 (1999).
[17]R. M. Galera, D. P. Osterman, J. D. Axe, S. Kunii, and T. Kasuya, J. Appl. Phys. **63**, 3580 (1988).
[18]K. Kuwahara, S. Sugiyama, K. Iwasa, M. Kohgi, M. Nakamura, Y. Inamura, M. Arai, and S. Kunii, Appl. Phys. A **74**, S302 (2002).
[19]M. Amara, S. E. Luca, R.-M. Galéra, F. Givord, C. Detlefs, and S. Kunii, Phys. Rev. B **72**, 064447 (2005).
[20]K. Kuwahara, R. Yamamoto, M. Kohgi, H. Nakao, K. Ishii, K. Iwasa, Y. Murakami, S. Kunii, H. Sagayama, Y. Wakabayashi, and H. Sawa, Phys. B **359–361**, 965 (2005).
[21]Z. Fisk, R. H. Taylor, and B. R. Coles, J. Phys. C **4**, 129 (1971).
[22]R. M. Galéra, P. Morin, S. Kunii, and T. Kasuya, J. Magn. Magn. Mater. **104**, 1336 (1992).
[23]J. P. Merculio, J. Etourneau, R. Naslain, and P. Hagenmuller, J. Less-Common Met. **41**, 175 (1976).
[24]S. Kunii, J. Phys. Soc. Jpn. **57**, 361 (1988).
[25]A. Q. R. Baron, Y. Tanaka, S. Goto, K. Takeshita, T. Matsushita, and T. Ishikawa, J. Phys. Chem. Solids **61**, 461 (2000); **69**, 3100 (2008).
[26]K. Iwasa, R. Igarashi, K. Saito, C. Laulhé, T. Orihara, S. Kunii, K. Kuwahara, H. Nakao, Y. Murakami, F. Iga, M. Sera, S. Tsutsui, H. Uchiyama, and A. Q. R. Baron, Chin. J. Phys. **49**, 231 (2011).
[27]S. Nakamura, T. Goto, S. Kunii, K. Iwashita, and A. Tamaki, J. Phys. Soc. Jpn. **63**, 623 (1994).
[28]M. Kohgi, K. Kuwahara, N. Ogita, M. Udagawa, and F. Iga, J. Phys. Soc. Jpn. **75**, 085003 (2006).
[29]S. Tsutsui, T. Hasegawa, Y. Takasu, N. Ogita, M. Udagawa, Y. Yoda, and F. Iga, J. Phys.: Conf. Ser. **176**, 012033 (2009).
[30]Y. Ishizawa, T. Tanaka, E. Bannai, and S. Kawai, J. Phys. Soc. Jpn. **42**, 112 (1977).
[31]A. Planes, E. Obradó, A. Gonzàlez-Comas, and L. Manosa, Phys. Rev. Lett. **79**, 3926 (1997).
[32]N. Singh, S. M. Saini, T. Nautiyal, and S. Auluck, J. Phys. Condens. Matter **19**, 346226 (2007).